

# Islands of stability of the $d$ -wave order parameter in $s$ -wave anisotropic superconductors

R. Gonczarek<sup>1</sup>, M. Krzyzosiak<sup>1,2,a</sup>, and A. Gonczarek<sup>3</sup>

<sup>1</sup> Institute of Physics, Wrocław University of Technology, Wybrzeże Wyspiańskiego 27, 50-370 Wrocław, Poland

<sup>2</sup> Department of Physics, Beijing Normal University, Beijing 100875, P.R. China

<sup>3</sup> Faculty of Fundamental Problems of Technology, and Faculty of Computer Science and Management, Wrocław University of Technology, Wybrzeże Wyspiańskiego 27, 50-370 Wrocław, Poland

Received 5 August 2007 / Received in final form 4 October 2007

Published online 22 February 2008 – © EDP Sciences, Società Italiana di Fisica, Springer-Verlag 2008

**Abstract.** In this paper we find and present on diagrams in the coordinates of  $\eta = 2t_1/t_0$  (the ratio of the second and the first nearest neighbor hopping integrals) and  $n$  (the carrier concentration) the areas of stability for the superconducting spin-singlet  $s$ - and  $d$ -wave and the spin-triplet  $p$ -wave order parameters hatching out during the phase transition from the normal to the superconducting phase. The diagrams are obtained for an anisotropic two-dimensional superconducting system with a relatively wide partially-filled conduction band. We study a tight-binding model with an attractive nearest neighbor interaction with the amplitude  $V_1$ , and the on-site interaction (with the amplitude  $V_0$ ) taken either as repulsive or attractive. The problem of the coexistence of the  $s$ -,  $p$ - and  $d$ -wave order parameters is addressed and solved for chosen values of the ratio  $V_0/V_1$ . A possible island of stability of the  $d$ -wave order parameter in the  $s$ -wave order parameter environment for a relatively strong on-site interaction is revealed. The triple points, around which the  $s$ -,  $d$ -, and  $p$ -wave order parameters coexist, are localized on diagrams. It is shown that results of the calculations performed for the two-dimensional tight-binding band model are dissimilar with some obtained within the BCS-type approximation.

**PACS.** 74.20.Rp Pairing symmetries (other than  $s$ -wave) – 74.62.Yb Other effects

## 1 Introduction

Superconducting high- $T_c$  systems, such as copper-oxides, with carriers within the  $\text{CuO}_2$  planes are usually regarded as a quasi two-dimensional system of fermions [1–5]. This is due to the characteristic, strongly anisotropic, layered structure of these materials with the symmetry of the  $\text{CuO}_2$  planes being the symmetry of the point group  $C_{4v}$  [6–10].

Such superconducting systems demand to take into account spin-fluctuations or strong-correlation effects, and can be described by means of an effective Hamiltonian of the strongly interacting Hubbard model with a given (multiband) one-particle dispersion relation enriched also by the self-energy corrections, and a quite general form of the pairing potential  $V(\mathbf{k}, \mathbf{k}')$  [4,11–15]. The pairing interaction can be decomposed into an antisymmetric and a symmetric part determining the spin-singlet ( $s$ - and  $d$ -wave) and the spin-triplet ( $p$ -wave) symmetry of the order parameter, respectively [16].

Acting in the spirit of the tight binding description we can assume that the overlap of the orbitals in differ-

ent unit cells is small, compared to the diagonal overlap values, thus the matrix element of  $V(\mathbf{k}, \mathbf{k}')$  may contain the on-site term, and the nearest neighbors and the further neighbors terms, which give rise to diverse wave-symmetry channels [17]. Since in the present paper we study the stability relations between the spin-singlet  $s$ - and  $d$ -wave and the spin-triplet  $p$ -wave order parameters with symmetry properties determined by the Fourier harmonics appearing in the expansion of the pairing potential into a double Fourier series, and the further neighbors terms correspond to higher order Fourier expansion coefficients [7,10], we focus on a model with an attractive nearest neighbor interaction with the amplitude  $V_1$  and an on-site interaction with the amplitude  $V_0$ , which can be taken either as repulsive or attractive. Moreover, we employ the one-particle band-structure reduced to a renormalized dispersion relation  $\xi_{\mathbf{k}}$  being a differentiable function of the momentum  $\mathbf{k}$  and fitted the parameters, whose symmetry corresponds to the symmetry group  $C_{4v}$  [1,2,4,7,16,18,19]. Although some possibilities of various superconducting symmetries including the effects of the  $\eta$ -ratio have been considered with regard to cuprates and ruthenates, and spreads of the domination of the  $p$ -wave or  $d$ -wave pairing states were outlined [20–22], the numerical results obtained in

<sup>a</sup> e-mail: mateusz.krzyzosiak@pwr.wroc.pl

the present paper determine stable regions of the order parameter for various values of the model parameters:  $\eta = 2t_1/t_0$  (the ratio of the second and the first nearest neighbor hopping integrals),  $n$  (the carrier concentration) and  $v = V_0/V_1$ . They display qualitative modifications of these stable regions implied by  $\eta$ ,  $n$  and  $v$  varying in their full acceptable range. The performed study points to some potentially global conditions of coexistence and stability of different superconducting states with a fixed symmetry.

Let us also note that considering the problem of coexistence of the spin-singlet  $s$ - and  $d$ -wave and the spin-triplet  $p$ -wave order parameters some authors also included a large spin-orbit coupling [23,24], as well as the broken inversion symmetry with antisymmetric spin-orbit coupling, which can contribute to the formation of particular states [25,26].

## 2 Employed formalism

Employing the Green function formalism one can find two basic equations, consistent with the mean-field approximation, i.e. the gap equation in the momentum space [6–9]

$$\Delta_{\mathbf{k}} = \sum_{\mathbf{k}'} V(\mathbf{k}, \mathbf{k}') \frac{\Delta_{\mathbf{k}'}}{E_{\mathbf{k}'}} \tanh \frac{E_{\mathbf{k}'}}{2T}, \quad (1)$$

where  $E_{\mathbf{k}} = \sqrt{(\xi_{\mathbf{k}} - \mu)^2 + \Delta_{\mathbf{k}}^2}$ , and another self-consistent equation

$$n = \frac{1}{N} \sum_{\mathbf{k}} \left( 1 - \frac{\xi_{\mathbf{k}} - \mu}{E_{\mathbf{k}}} \tanh \frac{E_{\mathbf{k}}}{2T} \right), \quad (2)$$

which determines the total chemical potential  $\mu = \mu_0 + \mu(T)$ . Here,  $\mu_0$  fixes the shift of the Fermi level due to doping and is a function of the conduction band filling  $n$  defined for the normal metallic phase at  $T = 0$ , whereas  $\mu(T)$  expresses its temperature correction ( $\mu(0) = 0$ ).  $N$  denotes the total number of lattice sites [16,19,27–29].

Since in anisotropic superconductors both the spin-singlet  $s$ -wave or  $d$ -wave symmetry states ( $S = 0, M = 0$ ) and the spin-triplet  $p$ -wave symmetry state ( $S = 1, M = 0$ ) can be formed, we investigate the impact of modifications in the shape of the dispersion relation taken in the tight-binding approach on stability of the above symmetry states. The influence of other factors, i.e. the carrier concentration  $n$ , and the pairing potential amplitudes  $V_0$  and  $V_1$  is also studied. In the present paper we consider a two-dimensional one-band model with a relatively wide partially-filled conduction band of the width  $2\omega$  and the dispersion relation taken in the form

$$\xi_{\mathbf{k}} = -2t_0(\cos k_x + \cos k_y + \eta \cos k_x \cos k_y), \quad (3)$$

where  $\eta = 2t_1/t_0$  and the case  $\eta = 0$  corresponds to the ideal nesting. The parameters  $t_0, t_1$  can be identified with the nearest-neighbor and the next-nearest-neighbor hopping integrals, respectively [30,31].

Superconductivity with anisotropic Cooper pairing has now to be defined and analyzed regarding the symmetry

based on the new quasiparticles, taking into consideration the generalized Ginzburg-Landau theory for unconventional superconductivity. However, the effective interaction between quasiparticles in strongly correlated systems is very complex as it in general depends on the spin and the current carried by quasiparticles. Since the conventional phonon-mediated pairing mechanism raises doubts — because of the expected magnetically mediated pairing mechanism, arising from the exchange of magnetic fluctuations — a generic, boson-mediated, strongly anisotropic attraction mechanism providing pairing interaction in the spin-antisymmetric and the spin-symmetric channels is included in the present study [1,3,4,19].

Considering the Fourier-transformed generic boson-mediated potential on a square lattice, we can assume that it is translational invariant and separable, so that the matrix element  $V(\mathbf{k}, \mathbf{k}')$  can be rewritten as

$$V(\mathbf{k}, \mathbf{k}') = V^s(\mathbf{k}, \mathbf{k}') + V^a(\mathbf{k}, \mathbf{k}'),$$

where the potentials  $V^s(\mathbf{k}, \mathbf{k}') = V^s(-\mathbf{k}, \mathbf{k}') = V^s(\mathbf{k}, -\mathbf{k}')$  and  $V^a(\mathbf{k}, \mathbf{k}') = -V^a(-\mathbf{k}, \mathbf{k}') = -V^a(\mathbf{k}, -\mathbf{k}')$ , refer to the spin-singlet and the spin-triplet pairing channels, respectively. Moreover, these components can be presented in separable forms

$$\begin{aligned} V^s(\mathbf{k}, \mathbf{k}') &= -V_0 - \sum_{j \geq 1, m} V_j^s f_{jm}(\mathbf{k}) f_{jm}(\mathbf{k}'), \\ V^a(\mathbf{k}, \mathbf{k}') &= - \sum_{j \geq 1, m} V_j^a g_{jm}(\mathbf{k}) g_{jm}(\mathbf{k}'). \end{aligned} \quad (4)$$

Then  $V_0$  and  $V_j^{s,a}$  are the amplitudes in the isotropic and anisotropic channels, corresponding to the on-site term, and the nearest neighbors and the further neighbors terms, respectively. The momentum-dependent functions  $f_{jm}(\mathbf{k}), g_{jm}(\mathbf{k})$ , for a given  $j$ , should be taken from proper subsets of normalized and orthogonal basis functions of irreducible representations of the group  $C_{4v}$  defined for a two-dimensional momentum space, including proper pairing channel symmetry [7,17]. Thus, their Fermi-surface-averages  $\langle f_{jm}^2(\mathbf{k}) \rangle = \langle g_{jm}^2(\mathbf{k}) \rangle = 1$  and  $\langle f_{jm}(\mathbf{k}) \rangle = \langle g_{jm}(\mathbf{k}) \rangle = 0$ , and  $\langle f_{im}(\mathbf{k}) f_{jn}(\mathbf{k}) \rangle = \langle g_{im}(\mathbf{k}) g_{jn}(\mathbf{k}) \rangle = 0$ , if  $i \neq j$  or  $m \neq n$ .

Instead, if the Fourier-transformed, specific boson-mediated potential, as e.g. in the magnetically mediated superconductivity [1], is given in the frequency and momentum representation including the translational invariance, then after projecting the pairing term on the previously defined subsets of the basis functions of irreducible representations of the group  $C_{4v}$  one should write down this pairing potential in the form (4). Note that the derived amplitudes can depend on frequency in the cutoff range of pairing (however rather as slowly-varying functions). Consequently, this approach seems to be less effective for models with interactions formulated in such a way.

In the present paper the studied boson-mediated pairing mechanism is assumed to take the phenomenological form reduced to isotropic on-site and anisotropic nearest-neighbor interactions on a two-dimensional square lattice, covering a relatively narrow region in the conduction

band. In the reciprocal space the pairing potential reads (here  $a_x = a_y = 1$ ) [4,32–35]

$$V(\mathbf{k}, \mathbf{k}') = -V_0 - V_1[\cos(k_x - k'_x) + \cos(k_y - k'_y)], \quad (5)$$

where the on-site potential with the amplitude  $V_0$  can be repulsive or attractive, whereas the nearest neighbor potential (amplitude  $V_1$ ) is always attractive, and they vanish beyond the cutoff energy  $\pm\omega_c$ . So, we consider a high- $T_c$  superconductor as a metallic system with a partially-filled conduction band and the pairing interaction in a confined region near to the Fermi level, and the additional phenomenological parameter  $v = V_0/V_1$  extends the range of application of the presented model. After some algebra the potential (5) can be transformed into the following separated forms [4,6–9,35]

$$V^s(\mathbf{k}, \mathbf{k}') = -V_0 - \frac{1}{2}V_1(\cos k_x + \cos k_y)(\cos k'_x + \cos k'_y) - \frac{1}{2}V_1(\cos k_x - \cos k_y)(\cos k'_x - \cos k'_y), \quad (6)$$

$$V^a(\mathbf{k}, \mathbf{k}') = -V_1(\sin k_x \sin k'_x + \sin k_y \sin k'_y) \quad (7)$$

compatible with irreducible representations of the group  $C_{4v}$  in the two-dimensional momentum space, and consistent with (4).

In order to perform detailed analytical and numerical calculations we employ the method of curvilinear transformations [7–9,16,18,19], which allows us to write down the fundamental equations (1) and (2) in a particular coordinate system  $(\xi, \varphi)$ , where  $\xi$  stands for the one-particle energy and  $\varphi$  is the angular variable of the standard polar coordinate system.

In the present paper we apply the formalism we have developed recently [9,18], which can be regarded as the extended Van Hove Scenario valid for superconducting systems with anisotropic pairing, maintaining the correct number of degrees of freedom in a two-dimensional reciprocal space. This formalism allows us to perform detailed analysis applying more convenient coordinate system. Consequently, the spin-singlet and spin-triplet pairing potentials can be then expanded in a double Fourier series in the angular variable. Since the spatial structure of the order parameter is determined by the dominating coefficient of the Fourier expansion, the symmetry of the order parameter can be identified with respect to the harmonic functions  $\sin n\varphi$  and  $\cos n\varphi$  [6–9,18,35,36].

The employed curvilinear transformation (the mathematical details are given in Ref. [7]) allows us to express the coordinates  $k_x, k_y$  as functions of  $\xi, \varphi$ , and eventually to replace the summation over quantum-mechanical states by the integration over  $\xi$  and  $\varphi$  according to the following formula

$$\sum_{\mathbf{k}} \dots = \int_{-\omega_c}^{\omega_c} d\xi \int_0^{2\pi} \frac{d\varphi}{2\pi} \mathcal{K}(\xi, \varphi) \dots,$$

where  $\mathcal{K}(\xi, \varphi) = \frac{2}{(2\pi)^2} \mathcal{J}(\xi, \varphi)$  (with  $\mathcal{J}$  being the Jacobian of the curvilinear transformation) can be treated as the kernel of the density of states corresponding to the local

deformation or modification of quantum-mechanical states in the  $(\xi, \varphi)$ -space. The coordinates  $k_x, k_y$  and the kernel of the density of states as functions of  $\xi, \varphi$ , for the tight-binding model with particle-hole asymmetry  $\eta$ , are of the forms [6–9,16,18,19]

$$k_x(\xi, \varphi, \eta) = \arccos \frac{1}{\eta} [X(\xi, \varphi, \eta) - 1],$$

$$k_y(\xi, \varphi, \eta) = \arccos \frac{1}{\eta} [Y(\xi, \varphi, \eta) - 1], \quad (8)$$

and

$$\mathcal{K}(\xi, \varphi, \eta) = \frac{\eta^2}{4\pi t_0} \frac{1}{\sqrt{\eta^2 - [X(\xi, \varphi) - 1]^2} \sqrt{\eta^2 - [Y(\xi, \varphi) - 1]^2}} \times \frac{1}{[X(\xi, \varphi)]^2 + [Y(\xi, \varphi)]^2} \frac{1}{1 + \sin 2\varphi} \phi_0(\xi), \quad (9)$$

where

$$X(\xi, \varphi, \eta) = \left[ \sqrt{\left(1 - \eta \frac{\xi}{2t_0}\right)^2 + \eta^2 \phi_0^2(\xi) f^2(\varphi) + \eta \phi_0(\xi) f(\varphi)} \right]^{\frac{1}{2}}$$

and

$$Y(\xi, \varphi, \eta) = \left[ \sqrt{\left(1 - \eta \frac{\xi}{2t_0}\right)^2 + \eta^2 \phi_0^2(\xi) f^2(\varphi) - \eta \phi_0(\xi) f(\varphi)} \right]^{\frac{1}{2}},$$

whereas

$$\phi_0(\xi, \eta) = \begin{cases} \frac{1}{2(1+\eta)^2} \left| 2 + \eta + \frac{\xi}{2t_0} \right| \left| 2 + 2\eta + \eta^2 - \eta \frac{\xi}{2t_0} \right| & \text{if } \frac{\xi}{2t_0} \leq \eta \\ \frac{1}{2(1-\eta)^2} \left| 2 - \eta - \frac{\xi}{2t_0} \right| \left| 2 - 2\eta + \eta^2 - \eta \frac{\xi}{2t_0} \right| & \text{if } \frac{\xi}{2t_0} \geq \eta \end{cases}$$

and

$$f(\varphi) = \frac{\sin \varphi - \cos \varphi}{\sin \varphi + \cos \varphi}.$$

Note that  $\phi_0(\xi, \eta) = \phi_0(-\xi, -\eta)$ ,  $X(\xi, \varphi, \eta) = Y(-\xi, \varphi, -\eta)$ , and  $\mathcal{K}(\xi, \varphi, \eta) = \mathcal{K}(-\xi, \varphi, -\eta)$ . The density of states can be then defined as [7–9,16,18,19]

$$\nu(\xi, \eta) = \frac{2}{\pi} \int_0^{\pi/2} d\varphi \mathcal{K}(\xi, \varphi, \eta), \quad (10)$$

and  $\nu(\xi, -\eta) = \nu(-\xi, \eta)$ .

In the case when one Fourier component dominates the others, the form of the symmetric (6) and the antisymmetric (7) components of the pairing potential, responsible for the formation of the spin-singlet,  $s$ - and  $d$ -wave, and the spin-triplet  $p$ -wave order parameters, respectively, read

1 pure  $s$ -wave pairing

$$V^s(\xi, \varphi; \xi', \varphi') = -V_0 - U_0(\eta, n) v_0(\xi, \eta, n) v_0(\xi', \eta, n),$$

2 pure  $p$ -wave pairing

$$V^a(\xi, \varphi; \xi', \varphi') = -2U_1(\eta, n) v_1(\xi, \eta, n) v_1(\xi', \eta, n) \times [\cos \varphi \cos \varphi' + \sin \varphi \sin \varphi'],$$

3 pure  $d$ -wave pairing

$$V^s(\xi, \varphi; \xi', \varphi') = -2U_2(\eta, n) v_2(\xi, \eta, n) \times v_2(\xi', \eta, n) \cos 2\varphi \cos 2\varphi',$$

where for  $l = 0, 1$ , or  $2$ ,  $v_l(\xi, \eta, n) = \chi_l(\xi, \eta) / \bar{\chi}_l(\eta, n)$ , the carrier concentration  $n = n(\eta, \mu_0)$  and

$$\bar{\chi}_l(\eta, n) = \frac{1}{2\omega_c} \int_{-\omega_c + \mu_0}^{\omega_c + \mu_0} \chi_l(\xi, \eta) d\xi$$

is the  $(\eta, n)$ -dependent mean value of the Fourier coefficient  $\chi_l(\xi, \eta)$  in the pairing region of the width  $2\omega_c$  (cf. Appendix A). The function  $U_l(\eta, n) = V_1 [\bar{\chi}_l(\eta, n)]^2$  defines the modified coupling coefficient for a particular pairing channel, satisfying the symmetry relation  $U_l(\eta, n(\eta, \mu_0)) = U_l(-\eta, n(-\eta, -\mu_0))$  for  $l = 0, 1$  and  $l = 2$ . Since the purely  $s$ -wave pairing potential is also modified (enhanced or diminished) by the constant term  $V_0$  corresponding to the on-site interaction, the  $s$ -wave symmetry superconducting state can gain the total stability for sufficiently large and positive  $V_0$  or it can be completely eliminated from the system for sufficiently large and attractive  $V_0$ .

Note that the separable forms 1–3 of the reduced pairing potential impose the following symmetry conditions on the order parameter:  $\Delta(\xi, \varphi, l, \eta, n) = \Delta(T) v_l(\xi, \eta, n) D(\varphi, l)$ , with

$$\begin{aligned} D(\varphi, 0) &= 1 && \text{for } s\text{-wave pairing} \\ D(\varphi, 1) &= \sqrt{2} \cos(\varphi + \beta_1) && \text{for } p\text{-wave pairing} \\ D(\varphi, 2) &= \sqrt{2} \cos 2\varphi && \text{for } d\text{-wave pairing} \end{aligned}$$

and solely  $\beta_1 = 0, \pm\pi/4, \pi/2$  should be included [7].

With regard to Fourier transformed generic boson-mediated potentials, the presented method of expanding the pairing potential in a double series of Fourier harmonics  $\sin n\varphi$  and  $\cos n\varphi$  has to be found to be more effective than the previously discussed, since the coefficients of the Fourier expansion define pairing amplitudes of a fixed symmetry. Consequently, in the case of magnetically mediated superconductivity [1], where spin-fluctuation modes contribute to the pairing amplitudes in the singlet and triplet channels in a different manner, the  $p$ -wave spin-triplet pairing appears in nearly ferromagnetic metals. On the other hand the  $d$ -wave spin-singlet pairing appears in nearly antiferromagnetic metals, what corresponds to the opposite values of one rigidly fixed parameter ( $\pm 2$ ). Thus, one can suspect that the  $p$ -wave and  $d$ -wave pairing amplitudes exchange domination when this rigidly fixed parameter takes the opposite value.

### 3 Analytical equations and numerical results

According to the experimental data [12,30,37–42] the dimensionless parameter  $\eta$  derived for the two-dimensional one-band tight-binding model for cuprate materials is negative and  $|\eta| \leq 0.9$ . On the other hand its value assessed for the two-dimensional  $t$ - $J$  model with an antiferromagnetic background, employing the quantum Monte Carlo method, is positive and can take values up to 1.53. Including  $t_0 = 0.24$  or  $0.35$  eV [30],  $\omega_c$  ranging from 26 meV to 65 meV [12], and employing the results of the local density approximation band structure calculations, where the band structure of YBCO was considered in the  $\epsilon_F \pm 2$  eV range [15], we may choose  $\omega_c/2t_0 \approx 0.1$  and  $\omega/\omega_c = 11$  for numerical evaluations. We also take into account that  $-0.9 \leq \eta \leq 0.9$ , and we demand the effective dimensionless pairing coefficient to satisfy the weak-coupling condition:  $\frac{1}{2} \nu_0(\eta) U_2(\eta) < 0.41$ . In the present study we focus on the cases when the pairing amplitude  $V_1/2\pi t_0 = 0.6, 1$  or  $1.9$ , and the ratio  $v = V_0/V_1$ , ranging between around  $-0.61$  and  $0.90$ , takes the following values:  $-0.25, 0, 0.25, 0.5, 0.6, 0.7$  and  $0.85$ . Moreover, the chosen conditions allow us to study some superconducting systems with a partially-filled conduction band when the chemical potential  $-1 \leq \mu_0/2t_0 \leq 1$ . Then the carrier concentration  $n$  can vary between the lower limit from  $0.02$  to  $0.14$  and the upper one from  $0.98$  to  $0.86$ .

The transformed equations (1) and (2) can be then applied to derive the order parameter amplitude  $\Delta(T)$  and the chemical potential  $\mu = \mu_0 + \mu(T)$  of the superconducting phase with the symmetry corresponding to  $l = 0, 1$  or  $2$ , for a fixed carrier concentration  $n$ .

In the  $T = T_c$  limit these equations can be written in the following reduced forms [7–9]

$$\begin{aligned} 1 &= [V_0 \delta_{0,l} + U_l(\eta, n)] \\ &\times \int_0^{2\pi} \frac{d\varphi}{2\pi} \int_{-\omega_c}^{\omega_c} d\xi \mathcal{K}(\xi + \mu_0, \varphi, \eta) \\ &\times \frac{D^2(\varphi, l)}{\xi - \mu(T_c)} \tanh \frac{\xi - \mu(T_c)}{2T_c}, \quad (11) \end{aligned}$$

where we assume that  $v_l(\xi + \mu_0, \eta) \cong 1$ . Consequently, equation (2) reads

$$\begin{aligned} n &= \frac{1}{N} \int_0^{2\pi} \frac{d\varphi}{2\pi} \int_{-\omega_c}^{\omega_c} d\xi \mathcal{K}(\xi, \varphi, \eta) \\ &\times \left[ 1 - \tanh \frac{\xi - \mu_0 - \mu(T_c)}{2T_c} \right]. \quad (12) \end{aligned}$$

Employing equation (2) in the limit  $T = 0$  one can evaluate relations among  $n$ ,  $\mu_0$  and  $\eta$  and find the carrier concentration  $n$  as a function of  $\eta$  and  $\mu_0$  for a fixed bandwidth  $2\omega$ . Then  $n(-\eta, \mu_0) = 1 - n(\eta, -\mu_0)$  [7–9].

In order to identify the regions of stability for  $s$ -,  $p$ -, and  $d$ -wave symmetry superconducting states on the  $(\eta, n)$  plane for the chosen values of  $V_0/V_1$  ratio and the fixed amplitude  $V_1$ , which are hatching out during the phase transition from the normal to superconducting phase, we compare the transition temperatures

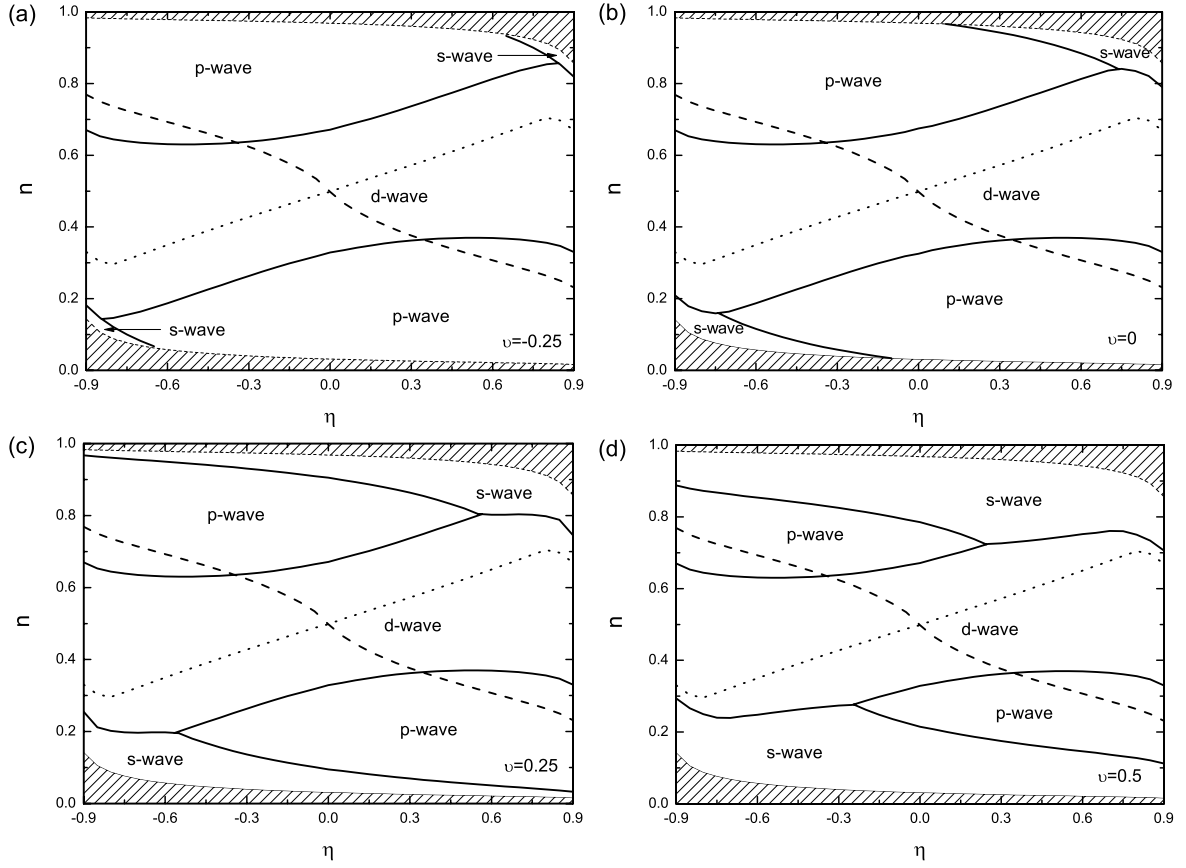


**Fig. 1.** The diagrams of stable spin-singlet  $s$ - and  $d$ -wave, and spin-triplet  $p$ -wave superconducting states obtained within the one-band tight-binding approach for various values of the  $v = V_0/V_1$  ratio: (a)  $v = -0.25$ , (b)  $v = 0$ , (c)  $v = 0.25$ , (d)  $v = 0.5$ . Supreme values of the transition temperature within the  $d$ -wave state stability area are attained along the dotted line. The half-filled conduction band ( $\mu_0/2t_0 = 0$ ) is denoted by the dashed line. Triple points positions are given in Table 1. In this and the following figures, the permitted region of the variables  $\eta$  and  $n$ , resulting from their relation to  $\mu_0$ , is shown as the unshaded area.

**Table 1.** The positions of triple points in the  $(\eta, n)$  diagrams estimated within the tight-binding approach for the chosen values of the  $v = V_0/V_1$  ratio.

$v$	-0.25	0	0.25	0.5	0.6
$(\eta, n)$	(-0.84, 0.14)	(-0.75, 0.16)	(-0.56, 0.20)	(-0.24, 0.28)	(0.046, 0.33)
$(\eta, n)$	(0.84, 0.86)	(0.75, 0.84)	(0.56, 0.80)	(0.24, 0.72)	(-0.046, 0.67)

$T_c(l, \eta, n)$  found self-consistently from equations (11) and (12) for fixed values of  $l$ ,  $\eta$  and  $\mu_0$ , applying recently developed methods [6–9,18,36]. According to the established relations the transition temperatures satisfy the relation  $T_c(l, -\eta, n(-\eta, \mu_0)) = T_c(l, \eta, n(\eta, -\mu_0))$  for  $l = 0, 1, 2$ .

In order to provide some reference for our results, we also employ the BCS-type approximation, where the kernel of the density of states  $\mathcal{K}(\xi, \varphi, \eta)$  is replaced by the average value of the density of states, i.e.

$$\nu_0(\eta) = \frac{1}{2\omega} \int_{-\omega_c}^{\omega_c} d\xi \nu(\xi, \eta), \quad (13)$$

then the transition temperature reads

$$T_{c0}(l, \eta, n) = \frac{2e^\gamma}{\pi} \omega_c \exp \left\{ -\frac{2}{\nu_0(\eta) [V_0 \delta_{0,l} + U_l(\eta, n)]} \right\}, \quad (14)$$

where  $\gamma \approx 0.577$  is the Euler constant, or  $T_{c0}(l, \eta, n) = 0$  if  $V_0 \delta_{0,l} + U_l(\eta, n) \leq 0$ . Moreover we have  $T_{c0}(l, -\eta, n(-\eta, \mu_0)) = T_{c0}(l, \eta, n(\eta, -\mu_0))$  for  $l = 0, 1, 2$ .

The diagrams in Figures 1 and 2 illustrate the common result obtained for three values of the pairing amplitude  $V_1/2\pi t_0 = 0.6, 1$ , or  $1.9$  after replacing  $\mu_0$  with  $n$  and mutual comparison of the transition temperatures  $T_c(0, \eta, n)$ ,  $T_c(1, \eta, n)$  and  $T_c(2, \eta, n)$ , when the values of the  $V_0/V_1$  ratio are equal to  $-0.25, 0, 0.25, 0.5, 0.6, 0.7$  and  $0.85$ , respectively. We emphasize that within the discussed model the boundary condition  $T_c(0, \eta, n) = T_c(1, \eta, n)$  coincides



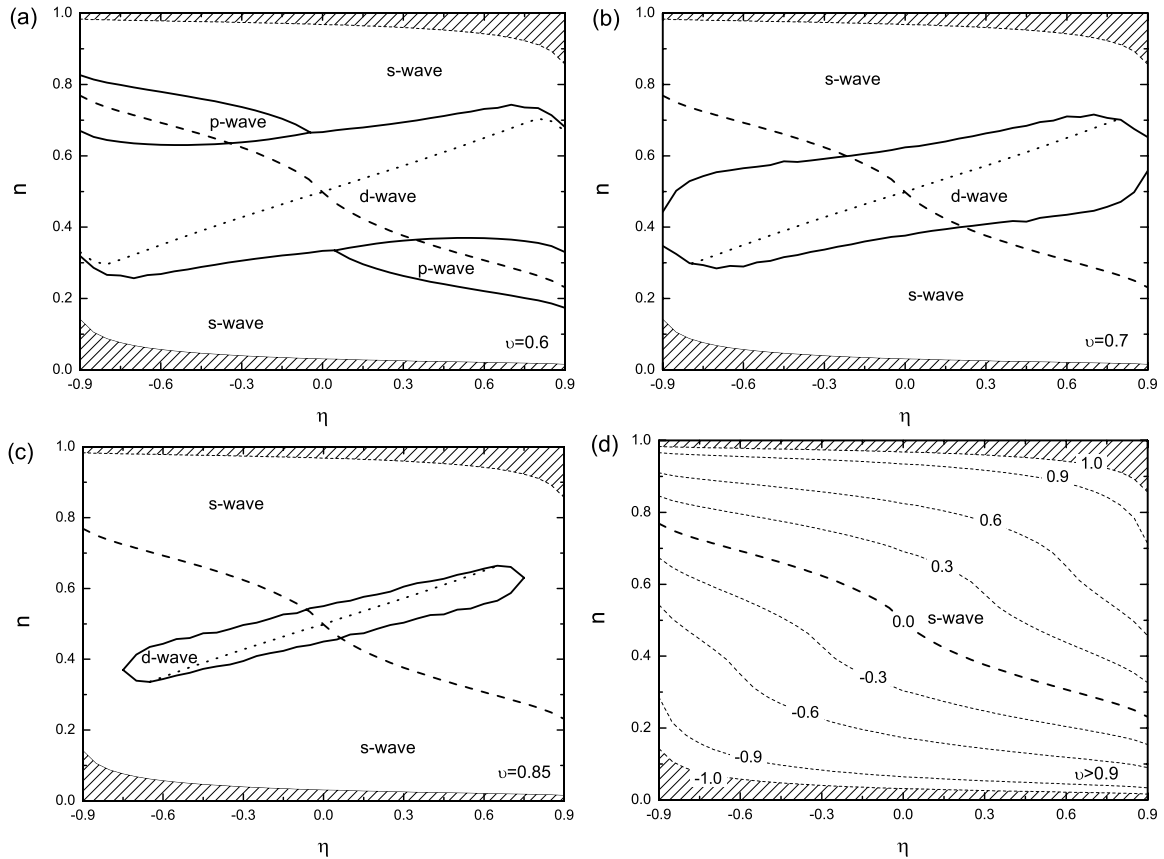


**Fig. 2.** Expulsion of the stable spin-singlet  $d$ -wave and the spin-triplet  $p$ -wave superconducting states from the diagrams by the spin-singlet  $s$ -wave superconducting state. Results obtained within the one-band tight-binding approach for various values of the  $\nu = V_0/V_1$  ratio. (a) The stability areas of the three discussed states for  $\nu = 0.6$  survive until  $\nu < 0.64$ . (b) The  $p$ -wave state has been eliminated ( $\nu = 0.7$ ). (c) The  $d$ -wave state for  $\nu = 0.85$  forms an island around the central point ( $\eta = 0, n = 0$ ) of the diagram. (d) Only the  $s$ -wave state can be realized in the system for  $\nu \geq 0.9$ . In (a–c) the supreme values of the transition temperature within the  $d$ -wave state stability areas are attained along the dotted line. The half-filled band concentration ( $\mu_0/2t_0 = 0$ ) is denoted by the dashed line. In (d) the equi-concentration lines for  $\mu_0/2t_0 = \pm 0.3, \pm 0.6, \pm 0.9, \pm 1.0$  have been additionally shown as thin dashed lines.

with the relation  $T_{c0}(0, \eta, n) = T_{c0}(1, \eta, n)$  for all values of  $\nu$  [7–9, 18].

The shape and the evolution of stability areas for particular order parameters show that the stable  $s$ -wave state appears on the diagram if  $\nu \geq -0.61$ , and it is preferred for the low and the high concentration  $n$  if  $\nu$  is negative, zero or positive (although small). The stability areas for the  $s$ -wave state expand when  $\nu$  increases (Figs. 1 and 2a), so that the  $p$ -wave state is eventually eliminated from the diagram for  $\nu \geq 0.64$  (cf. Figs. 2b–2d). The diminishing area of the stable  $d$ -wave state forms an island in the  $s$ -wave order parameter sea (as depicted in Fig. 2c), and occupies the central region of the diagram for  $\nu$  up to ca. 0.9. For larger values of  $\nu$  only the  $s$ -wave state can be realized in the system.

Since for the diagrams the stability areas for the  $s$ -wave,  $d$ -wave, and  $p$ -wave order parameters have been evaluated in the limit  $\Delta(T) \rightarrow 0$ , the pure-symmetry state exist in these areas only, which are separated from the others by phase transition lines. However, one can expect that in superconducting phase when the tempera-

ture  $T$  is very close to  $T_c(l, \eta, n)$ , the phase transition lines broaden proportionally to  $(T_c(l, \eta, n) - T)$ . Then one can find regions — near to the boundaries between the distinguished areas — where the spin-singlet  $s$ -wave and the spin-triplet  $p$ -wave or the spin-singlet  $d$ -wave and the spin-triplet  $p$ -wave, or the spin-singlet  $s$ -wave and the spin-singlet  $d$ -wave order parameters coexist (cf. Figs. 1 and 2).

On the diagrams there also appear triple points around which spin-singlet  $s$ -wave and the  $d$ -wave, and spin-triplet  $p$ -wave order parameters can coexist as in Figures 1 and 2a. Some estimated values of the triple points positions are given in Table 1. The supreme values of the transition temperature found for a given value of the parameter  $\eta$  are located along the dotted line in the  $d$ -wave order parameter region in Figures 1 and 2. Note that the dotted line always goes through the central point of diagrams ( $\eta = 0, n = 0$ ) and the highest transition temperatures are attained for the  $d$ -wave superconducting state.

In Figure 1 we present some cases when stability areas for  $s$ -wave,  $d$ -wave, and  $p$ -wave order parameters are revealed. They appear for  $-0.9 \leq \eta \leq 0.9$  and  $n_d < n < n_u$  where  $n_d = n(\eta, \mu_0/2t_0 = -1) > 0$  and  $n_u = n(\eta, \mu_0/2t_0 = 1) < 1$ . Stability areas for order parameters of various symmetry can be observed in the presented diagrams when  $-0.61 < v < 0.64$ .

In Figure 2 we display some cases, when stability areas for the  $d$ -wave and  $p$ -wave order parameters are eliminated from the diagrams by the  $s$ -wave order parameter. The stability areas for the  $p$ -wave order parameter remain on the diagram when  $v < 0.64$ , whereas stability areas for the  $d$ -wave order parameter survive until  $v = 0.9$ .

Calculations carried out based on the two-dimensional tight-binding band model allowed us to include the complex structure of the dispersion relation and the pairing potential treated within the conformal transformation approach [6–9,36]. The obtained results show that in the case of a nearly half-filled conduction band the spin-singlet  $d$ -wave symmetry superconducting state remains stable for small values of the parameter  $\eta$ , even for a strong attractive on-site interaction (Figs. 1 and 2). So, the  $d$ -wave state is able to compete with the  $s$ -wave one in some doped systems. In contrary to this approach the numerical results obtained within the BCS-type approximation by employing equation (14) reveal a strong domination of the  $s$ -wave state in the presence of an attractive on-site interaction (Fig. 3).

The more detailed calculations performed for the BCS-type approximation clearly illustrate how the stability areas of the  $s$ -wave order parameter gradually fill up the diagram with increasing attractive on-site interaction ( $V_0 > 0$ ), and how they are being eliminated when this interaction becomes repulsive ( $V_0 < 0$ ). The diagrams of stable superconducting states obtained for  $v = -0.25, 0, 0.25, 0.5, 0.6$  and  $v \geq 0.64$  are presented in Figure 3. The  $s$ -wave order parameter is stable in the whole diagram if  $v \geq 0.64$ , and it is completely eliminated from the diagram if  $v \leq -0.61$  [8,9]. The boundaries established between the stability areas of the  $s$ -wave and the  $p$ -wave order parameters partially coincide with some obtained for the tight-binding model, while the boundaries between stability areas for the  $p$ -wave and the  $d$ -wave order parameters keep their shape. This results in a shift of the triple points.

Since the transition temperatures depend on  $\eta$ ,  $n$ ,  $v$  and the order parameter symmetry, they vary essentially within the diagrams and amongst them. It allows us to argue that in some high- $T_c$  superconductors of similar molecular composition, different symmetry order parameters can be created during the phase transition. Moreover, the isotropic on-site interaction and the contributing anisotropic nearest-neighbor interactions can significantly modify the regions of order parameters stability.

Although the above considerations involve the case  $\Delta(T) \rightarrow 0$  and can be referred merely to the regions of temperatures very close to  $T_c(l, \eta, n)$ , which are the most intensively investigated experimentally, the developed for-

malism can be also employed to study stability of the order parameters for temperatures from 0 to  $T_c(l, \eta, n)$ .

Since  $\Delta(T)$  and  $\mu = \mu_0 + \mu(T)$ , for the specified symmetry of the order parameters and fixed  $n$ , can be derived from the transformed equations (1) and (2), independently [7], one can find the free energy difference employing some universal relations between the energy gap  $\Delta(T)$  and the thermodynamic potential difference defined between the superconducting and the normal phase [43], and the chemical potential of the superconducting phase. After comparison of the free energy differences for the given model parameters and temperature, one can identify a stable order parameter. However, such procedure is very arduous to perform for the imposed conditions.

## 4 Conclusions

Comparing the results of the tight-binding approach and those obtained for the simplified BCS-type approximation one should note the fundamental differences in the topology of the phase diagram with regard to the stability areas of the  $s$ -,  $p$ -, and  $d$ -wave order parameters, and their gradual evolution. The obtained results prove that the ratios  $v = V_0/V_1$  and  $\eta = 2t_1/t_0$ , as well as the carrier concentration  $n$ , have a crucial impact on values of the transition temperature for superconducting states of a fixed symmetry ( $s$ -,  $p$ - or  $d$ -wave).

Numerical calculations performed for the tight-binding band model point out that the spin-singlet  $d$ - or  $s$ -wave, and the spin-triplet  $p$ -wave symmetry superconducting states can be stable in large areas of the  $(\eta, n)$  plane for all values of  $\eta$  (i.e.  $|\eta| \leq 0.9$ ), if one fixes the carrier concentration  $n$  properly. The regions near to the boundary between the areas of stable states seem to be of special interest, because two different order parameters coexist there. With regard to the triple points, the observation of coexistence of the  $s$ -,  $d$ -, and  $p$ -wave order parameters could be possible for various doped samples if  $-0.61 \leq v \leq 0.64$  [7–9,12,44]. Beyond these limits the triple points are eliminated from the diagram and, eventually, the  $s$ -wave order parameter is being strongly suppressed or fully favored. We emphasize that the model parameters:  $\eta$ ,  $n$ ,  $v$  have a diverse and mutually competing influence on the values of transition temperatures. Hence, if the on-site interaction is attractive, the  $s$ -wave order parameter is stabilized in the whole diagram only when  $v \leq 0.64$  (cf. [21]).

Certainly, we do not insist that the tight-binding model results are quantitatively complete. Our aim was rather to display that by applying the presented calculation method to some other more composed models of high- $T_c$  superconductors, one should obtain qualitatively comparable results. Moreover, the triple point effects, and coexistence of the  $s$ -wave and the  $d$ -wave order parameters should be possible to observe in the delineated regions of the diagrams. We emphasize that one could not expect that the discussed model parameters (i.e.  $n$ ,  $\eta$ , and  $v$ ) can be modified in their full range under consideration in one composed superconducting system by doping and introducing impurities. However, there are

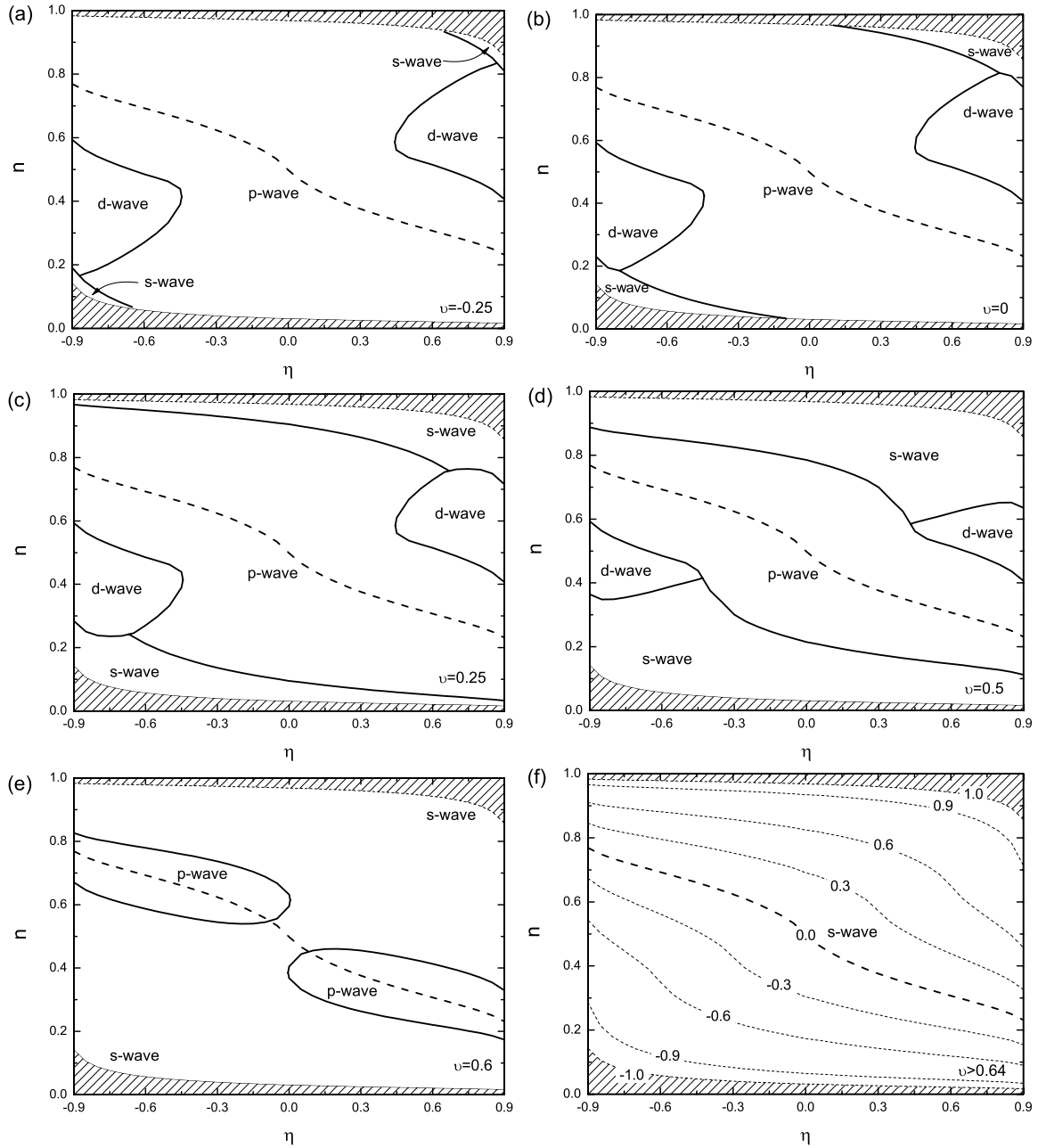


**Fig. 3.** (a) The diagram of stable spin-singlet  $s$ - and  $d$ -wave, and spin-triplet  $p$ -wave superconducting states obtained within the BCS-type approximation for various values of the  $v = V_0/V_1$  ratio: (a)  $v = -0.25$ , (b)  $v = 0$ , (c)  $v = 0.25$ , (d)  $v = 0.5$ , (e)  $v = 0.6$ , (f)  $v \geq 0.64$ . The half-filled band concentration ( $\mu_0/2t_0 = 0$ ) is denoted by the dashed line. In Figure f the equi-concentration lines for  $\mu_0/2t_0 = \pm 0.3, \pm 0.6, \pm 0.9, \pm 1.0$  have been additionally displayed as thin dashed lines.

many possibilities in experimental search for the discussed effects. For example, in the  $\text{YBa}_2\text{Cu}_3\text{O}_{6+x}$  compounds the metallic phase is formed by hole carriers roughly for  $x > 0.5$  and the increase in carrier concentration is implied by controlled oxygen doping. Since the superconducting state of the correlated pairs of holes is realized in the metallic phase regime, the points corresponding to various values of the parameter  $x$  (determining  $n$ ,  $\eta$  and  $v$ ), should be distributed in the diagrams presented in Fig-

ures 1 and 2 [30,45,46]. The most promising candidates seem to be variously doped superconducting compounds such as spinel- and perovskite-type structures of superconducting compounds of the type  $A_{2-y}B_y\text{CuO}_{4-x}$  and  $A_yB_{3-y}\text{Cu}_3\text{O}_{6+x}$ , where  $A$  is a trivalent rare-earth and  $B$  is a divalent alkali earth ion, as well as some recently studied novel superconducting compounds of  $\text{MgB}_2$  with a C, Al or Sc substitution, or organic superconductors with a controlled bandwidth and band filling [47–51].



Let us note that although the parameter  $\eta$  is fixed and constant for each superconducting sample, one can modify  $\eta$  by placing the sample in an uniform perpendicular magnetic field. Since we take into account the spin-triplet paired states with the spin projection  $S_z = 0$  and the spin-singlet paired states, which are affected by the magnetic field due to the Zeeman coupling, ineffectively, the Zeeman coupling leads solely to the renormalization of the chemical potential  $\mu \mapsto \bar{\mu} = \mu \pm \frac{1}{2}g\mu_B H$ . Thus, the magnetic field  $H$  moves singularities in  $\mathcal{K}(\xi, \varphi)$  and in the density of states away from the Fermi surface, and reduces the enhancement of the transition temperature [52]. Therefore, eventually, for sufficiently large  $H$  the field-induced transition from the spin-singlet to the spin-triplet superconductivity should be observed, as it has been reported recently [27].

Also note that many present experiments concentrate on structural and thermodynamic properties of novel compounds such as heavy fermion superconductors without a center of symmetry implying a non-centrosymmetric order parameter [25,26]. In such systems the broken inversion symmetry and the accompanying antisymmetric spin-orbit coupling, which admix spin-singlet and spin-triplet pairing, are proposed to be considered as responsible for such behavior, which should ensure quantitative agreement of the experimental data with the theory.

One of the authors (MK) is grateful to Professor Shiping Feng for his kind hospitality at the Department of Physics, Beijing Normal University. MK was supported by the China Scholarship Council (CSC No. 2007616032). A research scholarship from Wroclaw University of Technology is also gratefully acknowledged.

## Appendix A: Fourier coefficients

The symmetry of the separated parts of pairing potentials (6) and (7) corresponds to the group  $C_{4v}$ . Hence the the functions  $\cos k_x + \cos k_y$ ,  $\cos k_x - \cos k_y$ ,  $\sin k_x$  and  $\sin k_y$ , defined in the two-dimensional momentum space, can be expanded in the Fourier series in the  $(\xi, \varphi)$  space in accordance with the symmetry properties of the harmonic functions  $\sin n\varphi$  and  $\cos n\varphi$  [7]. Since the symmetry of this problem is determined by the symmetry of the dispersion relation (3), we state that  $k_x$  and  $k_y$  as functions  $\xi$ ,  $\varphi$  ( $0 \leq \varphi < 2\pi$ ), and  $\eta$ , can be expressed in two equivalent forms (cf. Eq. (8)):

$$k_x(\xi, \varphi, \eta) = \arccos \frac{1}{\eta} [X(\xi, \varphi, \eta) - 1],$$

$$k_y(\xi, \varphi, \eta) = \arccos \frac{1}{\eta} [Y(\xi, \varphi, \eta) - 1],$$

or

$$k_x(\xi, \varphi, \eta) = \arccos \frac{1}{\eta} [Y(\xi, \varphi, \eta) - 1],$$

$$k_y(\xi, \varphi, \eta) = \arccos \frac{1}{\eta} [X(\xi, \varphi, \eta) - 1],$$

what appears as a result of the symmetry of the canonical transformation  $k_i \mapsto \pi - k_i$ , where  $i = x, y$ , of exchange between  $(0, 0)$  and  $(\pi, \pi)$ . Hence, including that  $X(\xi, \varphi, \eta) = Y(-\xi, \varphi, -\eta)$  and  $X(\xi, \frac{\pi}{2} - \varphi, \eta) = Y(\xi, \varphi, \eta)$  one can notice that the canonical transformation implies that  $\eta$  as well as  $\xi$  must be replaced by  $-\eta$  and  $-\xi$ . The main Fourier expansion coefficients ( $l = 0, 1, 2$ ) can be written in the following reduced forms

$$\chi_0(\xi, \eta) = \frac{\sqrt{2}}{\pi} \int_0^{\pi/2} [\cos k_x(\xi, \varphi, \eta) + \cos k_y(\xi, \varphi, \eta)] d\varphi,$$

$$\chi_1(\xi, \eta) = \frac{\sqrt{2}}{\pi} \int_0^{\pi/2} [\sin k_x(\xi, \varphi, \eta) + \sin k_y(\xi, \varphi, \eta)] \cos \varphi d\varphi$$

$$= \frac{\sqrt{2}}{\pi} \int_0^{\pi/2} [\sin k_y(\xi, \varphi, \eta) + \sin k_x(\xi, \varphi, \eta)] \sin \varphi d\varphi$$

and

$$\chi_2(\xi, \eta) = \frac{2}{\pi} \int_0^{\pi/2} [\cos k_x(\xi, \varphi, \eta) - \cos k_y(\xi, \varphi, \eta)] \cos 2\varphi d\varphi,$$

where we allow for the symmetry arising from the canonical transformation, and we include that the basis functions of one-dimensional irreducible representations, as in cases  $l = 0$  and  $2$ , are transformed into one-dimensional subspaces of functions after the Fourier expansion, while projections of the basis functions of the two-dimensional irreducible representation,  $\{\sin k_x, \sin k_y\}$ , onto the two-dimensional subspace of the Fourier harmonics  $\{\cos \varphi, \sin \varphi\}$  have to be invariants of a possible choice of  $k_x(\xi, \varphi, \eta)$  and  $k_y(\xi, \varphi, \eta)$ . Consequently, the above Fourier expansion coefficients satisfy the identical conditions  $\chi_l^2(-\xi, -\eta) = \chi_l^2(\xi, \eta)$  for both possible choices of  $k_x(\xi, \varphi, \eta)$  and  $k_y(\xi, \varphi, \eta)$ .

## References

1. P. Monthoux, G.G. Lonzarich, Phys. Rev. B **59**, 14598 (1999); P. Monthoux, G.G. Lonzarich, Phys. Rev. B **63**, 054529 (2001); P. Monthoux, G.G. Lonzarich, Phys. Rev. B **66**, 224504 (2002)
2. A. Nazarenko, E. Dagotto, Phys. Rev. B **53**, R2987 (1996)
3. M. Sigist, K. Ueda, Rev. Mod. Phys. **63**, 239 (1991)
4. D.Y. Xing, M. Liu, Y.-G. Wang, J. Dong, Phys. Rev. B **60**, 9775 (1999)
5. S.P. Feng, Y. Song, Phys. Rev. B **55**, 642 (1997)
6. R. Gonczarek, M. Krzyzosiak, Physica C **426**, 278 (2005)
7. R. Gonczarek, L. Jacak, M. Krzyzosiak, A. Gonczarek, Eur. Phys. J. B **49**, 171 (2006)
8. R. Gonczarek, M. Krzyzosiak, L. Jacak, A. Gonczarek, Phys. Stat. Sol. (b) **244**, 3559 (2007)
9. M. Krzyzosiak, R. Gonczarek, A. Gonczarek, L. Jacak, *Conformal Transformation Method in Studies of High- $T_c$  Superconductors — Beyond the Van Hove Scenario*, in *Superconductivity Research Trends* (Nova Science Publishers, Hauppauge, New York, 2007), in press

10. R. Gonczarek, M. Krzyzosiak, *Model of Superconductivity in the Singular Fermi Liquid* in: *Progress in Superconductivity Research* (Nova Science Publishers, Hauppauge, New York, 2007), in press
11. F.C. Zhang, T.M. Rice Phys. Rev. B **37**, 3759 (1988)
12. R. Micnas, J. Ranniger, S. Robaszkiewicz, Rev. Mod. Phys. **62**, 113 (1990)
13. E. Pavarini, I. Dasgupta, T. Saha-Dasgupta, O. Jepsen, O.K. Andersen, Phys. Rev. Lett. **87**, 047003 (2001)
14. G. Litak, Phys. Stat. Sol. (b) **229**, 1427 (2002)
15. O.K. Andersen, A.I. Liechtenstein, O. Jepsen, F. Paulsen, J. Phys. Chem. Solids **56**, 1573 (1995); O.K. Andersen, S.Y. Savrasov, O. Jepsen, A.I. Liechtenstein, J. Low Temp. Phys. **105**, 285 (1996)
16. R. Gonczarek, M. Gładysiewicz, M. Mulak, Int. J. Mod. Phys. B **15**, 491 (2001)
17. H. Ghosh, J. Phys.: Condens. Matter **11**, L371 (1999)
18. R. Gonczarek, M. Krzyzosiak, M. Mulak, J. Phys. A **37**, 4899 (2004)
19. R. Gonczarek, M. Gładysiewicz, M. Mulak, Phys. Stat. Sol. (b) **233**, 351 (2002)
20. P. Monthoux, G.G. Lonzarich, Phys. Rev. B **71**, 054504 (2005)
21. T. Nomura, K. Yamada, J. Phys. Soc. Jpn **69**, 3678 (2000); T. Nomura, K. Yamada, J. Phys. Soc. Jpn **71**, 1993 (2002)
22. H. Fukazawa, K. Yamada, J. Phys. Soc. Jpn **71**, 1541 (2000)
23. K.K. Ng, M. Sigrist, Europhys. Lett. **49**, 473 (2000)
24. J.F. Annett, G. Litak, B.L.Györfy, K.I. Wysokiński, Phys. Rev. B **73**, 134501 (2006)
25. E. Bauer, G. Hilscher, H. Michor, Ch. Paul, E.W. Scheidt, A. Griбанov, Yu. Seropugin, H. Noël, M. Sigrist, P. Rogl, Phys. Rev. Lett. **92**, 027003 (2004)
26. H.Q. Yuan, D.F. Agterberg, N. Hayashi, P. Badica, D. Vandervelde, K. Togano, M. Sigrist, M.B. Salamon, Phys. Rev. Lett. **97**, 017006 (2006)
27. M.M. Maška, M. Mierzejewski, B. Andrzejewski, M.L. Foo, R.J. Cava, T. Klimczuk, Phys. Rev. B **70**, 144516 (2004)
28. J. Bouvier, J. Bok, *The Gap Symmetry and Fluctuations in High  $T_c$  Superconductors*, edited by J. Bok, G. Deutscher, D. Pavuna, S. Wolf (Plenum Press, New York, 1998), p. 37
29. R. Baquero, D. Quesada, C. Trallero-Giner, Physica C **271**, 122 (1996)
30. R.S. Markiewicz, J. Phys. Chem. Solids **58**, 1179 (1997)
31. H.Q. Lin, J.E. Hirsch, Phys. Rev. B **35**, 3359 (1987)
32. H. Shimahara, S. Hata, Phys. Rev. **62**, 14541 (2000)
33. J. González, Phys. Rev. B **63**, 024502 (2000)
34. E.Ya. Sherman, Phys. Rev. B **58**, 14187 (1998)
35. Q. Yuan, P. Thalmeier, Phys. Rev. B **68**, 174501 (2003)
36. R. Gonczarek, M. Krzyzosiak, Acta Phys. Polon. A **109**, 493 (2006)
37. C.C. Tsuei, D.M. Newns, C.C. Chi, P.C. Pattanaik, Phys. Rev. Lett. **65**, 2724 (1990); C.C. Tsuei, D.M. Newns, C.C. Chi, P.C. Pattanaik, Phys. Rev. Lett. **68**, 1091 (1992)
38. E. Dagotto, A. Nazarenko, M. Boninsegni, Phys. Rev. Lett. **73**, 728 (1994); E. Dagotto, Rev. Mod. Phys. **66**, 763 (1994); E. Dagotto, A. Nazarenko, A. Moreo, Phys. Rev. Lett. **74**, 310 (1995)
39. J.M. Getino, M. de Llano, H. Rubio, Phys. Rev. B **48**, 597 (1993); J.M. Getino, M. de Llano, H. Rubio, Phys. Rev. B **48**, 597 (1993)
40. R.S. Markiewicz, Physica C **168**, 195 (1990); R.S. Markiewicz, Physica C **183**, 303 (1991)
41. R.S. Markiewicz, C. Kusko, V. Kidambi, Phys. Rev. B **60**, 627 (1999)
42. H.H. Fertwell, A. Kaminski, J. Mesot, J.C. Campuzano, M.R. Norman, M. Randeria, T. Sato, R. Gatt, T. Takahashi, K. Kadowaki, Phys. Rev. Lett. **84**, 4449 (2000); S.V. Borisenko, M.S. Golden, S. Legner, T. Pichler, C. Dürr, M. Knupfer, J. Fink, G. Yang, S. Abell, H. Berger, Phys. Rev. Lett. **84**, 4453 (2000)
43. R. Gonczarek, M. Krzyzosiak, Phys. Stat. Sol. (b) **238**, 29 (2003)
44. K. Kuboki, J. Phys. Soc. Jpn **70**, 2698 (2001)
45. M. Cyrot, D. Pavuna, *Introduction to Superconductivity and High- $T_c$  Materials* (World Scientific Publ. Co., London, New Jersey, Singapore, Hong Kong, Bangalore, Beijing, 1992), Chap. 7.1
46. P.W. Anderson, Science **288**, 480 (2000)
47. R. Gonczarek, Appl. Phys. A **47**, 111 (1988)
48. D. Kasinathan, K.-W. Lee, W.E. Pickett, Physica C **424**, 116 (2005)
49. J. Kortus, O.V. Dolgov, R.K. Kremer, A.A. Golubov, Phys. Rev. Lett. **94**, 027002 (2005)
50. W.S. Agrestini, C. Metallo, M. Filippi, L. Simonelli, G. Campi, C. Sanipoli, E. Liarokapis, S. De Negri, M. Giovannini, A. Saccone, A. Latini, A. Bianconi, Phys. Rev. B **70**, 134514 (2004)
51. H. Mori, H. Mori, T. Okano, M. Kamiya, M. Haemori, H. Suzuki, S. Tanaka, Y. Nishio, K. Kajita, H. Moriyama, Physica C **357-360**, 103 (2001)
52. R. Gonczarek, M. Mulak, Phys. Lett. A **251**, 262 (1999)